

Received February 13, 2019, accepted February 25, 2019, date of publication March 1, 2019, date of current version March 20, 2019.

Digital Object Identifier 10.1109/ACCESS.2019.2902521

Linear, Quadratic, and Semidefinite Programming Massive MIMO Detectors: Reliability and Complexity

RAFAEL MASASHI FUKUDA AND TAUFIK ABRÃO¹, (Senior Member, IEEE)

Electrical Engineering Department, State University of Londrina, Londrina 86057-970, Brazil

Corresponding author: Taufik Abrão (taufik@uel.br)

This work was supported in part by the National Council for Scientific and Technological Development (CNPq) of Brazil under Grant 304066/2015-0, in part by the State University of Londrina (UEL), and in part by the State Government of Parana.

ABSTRACT One of the downsides of the massive multiple-input-multiple-output (M-MIMO) system is its computational complexity. Considering that techniques and different algorithms proposed in the literature applied to conventional MIMO may not be well suited or readily applicable to M-MIMO systems, in this paper, the application of different formulations inside the convex optimization framework is investigated. This paper is divided into two parts. In the first part, linear programming, quadratic programming (QP), and semidefinite programming are explored in an M-MIMO environment with high-order modulation and under realistic channel conditions, i.e., considering spatial correlation, error in the channel estimation, as well as different system loading. The bit error rate is evaluated numerically through Monte Carlo simulations. In the second part, algorithms to solve the QP formulation are explored, and computational complexity in terms of floating-point operations (flops) is compared with linear detectors. Those algorithms have interesting aspects when applied to our specific problem (M-MIMO detection formulated as QP), such as the exploitation of the structure of the problem (*simple constraints*) and the improvement of the rate of convergence due to the well-conditioned Gram matrix (channel hardening). The number of iterations is higher when the number of users K becomes similar to the number of base station antennas M (i.e., $K \approx M$) than the case $K \ll M$; the number of iterations increases slowly as the number of users K and base station antennas M increases while keeping a low system loading. The QP with projected algorithms presented better performance than minimum mean square error detector when $K \approx M$ and promising computational complexity for scenarios with increasing K and low system loading.

INDEX TERMS Massive MIMO communication, low-complexity detectors, convex optimization, linear programming, quadratic programming, semidefinite programming.

I. INTRODUCTION

Multiple input multiple output (MIMO) system with large number of antennas, often called Massive MIMO (M-MIMO), or even large-scale MIMO (LS-MIMO), is a promising technology where the great number of antennas provides several advantages, such as improved energy and spectrum efficiency, disappearance of thermal and fading noise effects [1], [2], to name a few.

However, among the benefits, new problems arise. One of the challenges in M-MIMO is the computational complexity

The associate editor coordinating the review of this manuscript and approving it for publication was Jiayi Zhang.

required to process the information from the great number of antennas [2], [3]. This problem is even more accentuated in the case of detection which is known for being a non-polynomial (NP-hard) problem with optimal brute force solution given by the maximum likelihood (ML) detector that is unfeasible even for a not so high number of antennas, users and modulation order combinations.

Although there are many techniques applied for *conventional* MIMO, such as linear detectors with matched filter (MF), zero forcing (ZF), minimum mean square error (MMSE), tree-search based algorithms including sphere decoding (SD), heuristics, detectors-based on convex optimization approach, and the possibility to combine with

transmit preprocessing techniques, e.g. precoding and coding to further improve the performance, detection is still an active field because most of the available algorithms apply to conventional MIMO systems and may not be well suited or readily applicable for M-MIMO systems (such as ML and SD) [3]. Hence, new and innovative detection algorithms must explore some of the specific features of M-MIMO structure.

In a multiuser M-MIMO scenario with low number of users and large number of antennas, linear detectors such as ZF and MF are known for providing near-optimal performance [4]. Some algorithms try to explore the channel hardening feature of the M-MIMO system that results in a well-conditioned Gram matrix $\mathbf{H}^H \mathbf{H}$ [4], [5] approximating the matrix inversion operation using techniques such as Neumann series [6], the Gauss-Seidel algorithm [7], and variations considering Newton algorithm such as [8], [9], and Newton-Schultz [10]. However, in those scenarios, a very small number of users K limits the potential gains in spectral efficiency since the capacity is proportional to the minimum between K and base station antennas M , i.e., $\min(K, M)$ [5] and, as the number of users increases, as in ultra-crowded heterogeneous machine type communication (mTC) and enhanced mobile broadband (eMBB) scenarios, the reliability and the performance of such detectors deteriorate [8], [11].

Another strategy to avoid the ML solution is the use of convex optimization algorithms, such as linear programming (LP) [12], [13], quadratic programming (QP) [14]–[16] and semidefinite programming (SDP) [17]–[20]. With the relaxation of some constraints, detectors can be formulated as convex optimization problems taking advantage of its solid theory and extensive literature (e.g., [21]–[23]) and making use of well-known polynomial-time algorithms [24], many of them conceived and applied to solve large scale problems [25]–[27].

Regarding LP, a detection scheme is investigated considering the ℓ_1 -norm in conventional MIMO scenario with 8×8 antennas in [12]. The detection problem is reformulated first as a mixed integer linear programming (MILP) and after, the discrete constraint is relaxed and the problem is cast into LP, which can be solved using interior point methods.

Zhang *et al.* [15] use a QP detector in an Orthogonal Frequency Division Multiplexing (OFDM) context aiming to reduce the interference among subcarriers, while Elghariani and Zoltowski [14] compare a QP and two other modified QP detectors with heuristics LAS and RTS (heuristics are not the focus of our paper) in an M-MIMO context. Although authors consider spatial correlation and different modulation orders, they do not explore error in the channel estimation and different system loading scenario.

The SDP detector is well-known in the literature and provides good performance results with an increased computational cost. The formulation in [17] is simple compared with other approaches [20]; it was tested for 16×16 MIMO system [17], for a 40×40 system [18], and for 128×128

in [19], however only considering a symmetric system with same number of antennas.

In order to solve LP, QP and SDP, interior-point algorithms can be applied [22], [23]. Particularly, the Mehrotra's Predictor Corrector (MPC) is the usual choice, and has been implemented in commands *linprog*, *lsqlin* in Matlab [28]–[30] to solve LP and QP, and in SDP3 to solve SDP [31]. Generally, interior-point methods involve the solution of a linear system of equations, hence have similar computational complexity order compared to linear detectors [14], and even greater in the case of SDP [18], [32].

General purpose solvers might be computationally expensive [27]; some algorithms are created considering the structure of the formulated problem, for example, the Two Metric Projection (TMP) [33] proposed to solve problems with *simple* constraints, such as nonnegative and box constraints [25]. With different scaling matrices, the TMP can become a Projected Gradient (PG) [26] or Projected Newton (PN) [25] algorithm (which are referred throughout the text as projected algorithms). TMP is capable to solve constrained problems similarly as its unconstrained counterpart and has advantages over manifold suboptimization and active set algorithms that require at least the number of constraints to converge [25]. Some application of those projected algorithms include large-scale problems arising in the machine learning field [26], quasi-Newton variations applied to image deblurring examples [27] and PG applied in beamforming [34].

This work is structured in two parts: in the first, the performance of different detectors formulated as optimization problems LP, QP and SDP in an M-MIMO context are studied in a variety of scenarios. In the second part, observing that the QP formulation presents the least number of variables, projected algorithms are applied to solve the QP formulation and its characteristics observed through numerical simulations.

The *contributions* of this work are threefold. **a)** An M-MIMO detector based on LP formulation is proposed using ℓ_∞ -norm (LP ℓ_∞), and its performance-complexity trade-off is compared with LP ℓ_1 -norm (originally proposed in [12] for conventional MIMO systems), QP and SDP-based detectors. Those detectors are considered in the new large scale MIMO context operating under realistic scenarios composed by channel correlation, error in the channel state information (CSI) estimation, and different number of users, including ($K \ll M$) and crowded scenarios ($K \approx M$), and also under different modulation orders. **b)** In the second part of the work, we focus on the application of projected algorithms to solve specifically the QP due to its reduced problem size compared with LP and SDP formulations and suitable performance. We characterize the application of solvers for QP and unveils the influence of the condition number of the Gram matrix (channel hardening effect) on the rate of convergence through numerical simulations. **c)** We have characterized both the convergence and complexity-performance trade-off of the proposed efficient

M-MIMO detectors compared with the linear detectors under different system loading.

Our work differs from others presented in the literature; for instance, in [35], the Newton’s Method (NM) is applied to LS-MIMO detection considering an optimization problem formulation where the constraints are discarded, hence solving an *unconstrained* problem. Herein, we use TMP and variations including PN, an algorithm adapted to solve *constrained* problems. In [8]–[10], NM and Newton-Schultz iterative algorithms are applied to M-MIMO detection problems in order to approximate the inverse of the channel matrix; however, differently from these approaches, we focus on the solution of an optimization problem.

The remainder of this paper is organized as follows. In section II the system model is described. Mathematical formulation of LP ℓ_1 , LP ℓ_∞ , QP, SDP-based M-MIMO detectors are presented in section III. Specific algorithms (solvers) applied to solve the optimization formulations LP, QP and SDP are detailed in section IV. Simulation results are divided in two parts. In the first part, the performance of the detectors are analyzed in subsection V-A, while the characterization and performance of projected algorithms are presented in subsection V-B. Computational complexity are analyzed in section VI. Final remarks and conclusions are offered in section VII.

Notation: bold lower case and bold upper case letters \mathbf{a} , \mathbf{A} represent column vectors and matrices, respectively. The i th element of vector is written in italic a^i , bold numbers denote a vector of the number (for example $\mathbf{3} = [3 \dots 3]^T$), and \mathbf{I} is the identity matrix.

II. UL M-MIMO SYSTEM MODEL

Considering a real-valued representation of an uplink (UL) M-MIMO system operating in multiplexing mode with single-antenna multiuser transmitters given by:

$$\mathbf{y} = \mathbf{H}\mathbf{x} + \mathbf{z}, \tag{1}$$

where \mathbf{y} and $\mathbf{z} \in \mathbb{R}^{2M}$, $\mathbf{x} \in \mathbb{R}^{2K}$ and $\mathbf{H} \in \mathbb{R}^{2M \times 2K}$ represent the received signal, additive noise with variance σ_z^2 , transmitted information and channel matrix, respectively; K represent number of user equipments (UEs), and M is the number of base station (BS) antennas.

In real applications, the separation between antennas can be smaller than half of the wavelength of the signal and spatial antenna correlation may occur [36]. Here we consider a uniform linear array (ULA) and the Kronecker model [36]; the correlated channel matrix is given by

$$\mathbf{H} = \sqrt{\mathbf{R}_M} \underline{\mathbf{H}} \sqrt{\mathbf{R}_K}, \tag{2}$$

where $\underline{\mathbf{H}}$, \mathbf{R}_M and \mathbf{R}_K represent the small-scale fading matrix with independent and identically distributed (iid) entries, the correlation matrices of the BS and UE, respectively. In the multiuser scenario considered, the Toeplitz symmetric matrix

\mathbf{R}_M is given by [37]

$$\mathbf{R}_M = \begin{bmatrix} 1 & \dots & \rho^{(M-1)^2} \\ \vdots & \ddots & \vdots \\ \rho^{(M-1)^2} & \dots & 1 \end{bmatrix}, \tag{3}$$

where $\rho \in [0, 1]$ is the correlation factor and here $\mathbf{R}_K = \mathbf{I}$, because users are autonomous and far from each other and, hence, not spatially correlated. Note that inside an uncorrelated scenario, $\mathbf{H} = \underline{\mathbf{H}}$.

Moreover, errors in the channel estimation are also considered as [38]

$$\tilde{\mathbf{H}} = \sqrt{1 - \tau^2} \mathbf{H} + \tau \mathbf{N}, \tag{4}$$

where $\mathbf{N} \sim \mathcal{N}(0, 1)$ and $\tau \in [0, 1]$ is the channel estimation quality parameter; for instance, $\tau = 0$ represents perfect knowledge of CSI, $\tau = 0.1$ means deviation of 10% in average from the perfect channel estimation.

III. M-MIMO DETECTORS

In order to recover the transmitted information, the ML detector denoted as the optimization problem

$$\begin{aligned} & \underset{\mathbf{x}}{\text{minimize}} \|\mathbf{y} - \mathbf{H}\mathbf{x}\|_p^2 \\ & \text{s.t. } \mathbf{x} \in \mathcal{B} \end{aligned} \tag{5}$$

can be applied. The symbol \mathcal{B} is related to the digital modulation and represents the set of constellation symbols (for a numerical example, 16-QAM has $\mathcal{B} = \{\pm 1; \pm 3\}$ in the equivalent real-valued representation) and p denotes the norm.

A. QUADRATIC PROGRAMMING

Equation (5) is an integer programming problem; in order to solve it, the usual approach (e.g. [12], [15], [17]) is to relax the integer constraint into a bound constraint considering \mathbf{x} a continuous variable. This results in a QP with linear (affine) inequalities

$$\begin{aligned} & \underset{\mathbf{x}}{\text{minimize}} \|\mathbf{y} - \mathbf{H}\mathbf{x}\|_{p=2}^2 \\ & \text{s.t. } \mathbf{b}_1 \leq \mathbf{x} \leq \mathbf{b}_2, \end{aligned} \tag{6}$$

which, opening the quadratic term of the objective function and reorganizing the constraints, becomes the problem

$$\begin{aligned} & \underset{\mathbf{x}}{\text{minimize}} \mathbf{x}^T \mathbf{H}^T \mathbf{H} \mathbf{x} - 2\mathbf{y}^T \mathbf{H} \mathbf{x} \\ & \text{s.t. } \begin{bmatrix} \mathbf{I} \\ -\mathbf{I} \end{bmatrix} \mathbf{x} \leq \begin{bmatrix} \mathbf{b}_2 \\ -\mathbf{b}_1 \end{bmatrix} \end{aligned} \tag{7}$$

where the term $\mathbf{y}^T \mathbf{y}$ is omitted from the objective function because it does not change the optimal point, $\mathbf{b}_1 \in \mathbb{R}^{2K}$ and $\mathbf{b}_2 \in \mathbb{R}^{2K}$ are vectors of the lower and upper values of the set \mathcal{B} with $\mathbf{b}_1 \leq \mathbf{b}_2$ (for example in 16-QAM, $\mathbf{b}_1 = -\mathbf{3}$ and $\mathbf{b}_2 = \mathbf{3}$). The problem in (6) is a QP, and can also be called constrained least squares (CLS) [21] problem or box constrained QP (BCQP) [39]. Problem (6) is the minimization of a quadratic function of \mathbf{x} with Hessian in the form of a symmetric and semidefinite positive Gram matrix $\mathbf{H}^T \mathbf{H}$ over

a convex set (i.e., a polyhedron, which is the intersection of a finite number of halfspaces and hyperplanes),¹ and hence, constitutes a convex optimization problem that can be solved using well-known algorithms. Notice that when the Hessian is indefinite, the problem is nonconvex and can have stationary points and/or local minima [23], [39], [41].²

B. LINEAR PROGRAMMING

Observing that the norm operator is always nonnegative and minimize the norm is equivalent to minimize the square of the norm [21], the optimization problem (6) can be equivalently expressed as

$$\begin{aligned} & \underset{\mathbf{x}}{\text{minimize}} \quad \|\mathbf{y} - \mathbf{H}\mathbf{x}\|_p \\ & \text{s.t.} \quad \mathbf{b}_1 \leq \mathbf{x} \leq \mathbf{b}_2. \end{aligned} \tag{8}$$

The problem (8) can be recast as LP in two different ways depending on the norm, namely sum of absolute residuals approximation for ℓ_1 norm ($p = 1$) and Chebyshev approximation for ℓ_∞ norm ($p = \infty$) [21].

1) LP WITH ℓ_1 -NORM

The detection problem (8) can be expressed in the LP form [12]

$$\begin{aligned} & \underset{\mathbf{x}, \mathbf{t}}{\text{minimize}} \quad \mathbf{1}^T \mathbf{t} \\ & \text{s.t.} \quad -\mathbf{t} \leq \mathbf{y} - \mathbf{H}\mathbf{x} \leq \mathbf{t} \\ & \quad \mathbf{b}_1 \leq \mathbf{x} \leq \mathbf{b}_2, \end{aligned} \tag{9}$$

where variables in the vector $\mathbf{t} \in \mathbb{R}^{2M}$ are the new optimization variables, jointly with the original variables \mathbf{x} .

Many solvers accept LP problems in a specific format such as equality or inequality form. Redefining variables, problem (9) can be expressed in the LP *standard inequality form*

$$\begin{aligned} & \underset{\mathbf{x}_{\ell_1}}{\text{minimize}} \quad \mathbf{c}_{\ell_1}^T \mathbf{x}_{\ell_1} \\ & \text{s.t.} \quad \mathbf{A}_{\ell_1} \mathbf{x}_{\ell_1} \leq \mathbf{b}, \end{aligned} \tag{10}$$

where

$$\begin{aligned} \mathbf{c}_{\ell_1} &= \begin{bmatrix} \mathbf{0} \\ \mathbf{1} \end{bmatrix}, \quad \mathbf{A}_{\ell_1} = \begin{bmatrix} \mathbf{H} & -\mathbf{I} \\ -\mathbf{H} & -\mathbf{I} \\ \mathbf{I} & \mathbf{0} \\ -\mathbf{I} & \mathbf{0} \end{bmatrix}, \quad \mathbf{x}_{\ell_1} = \begin{bmatrix} \mathbf{x} \\ \mathbf{t} \end{bmatrix}, \\ \mathbf{b} &= \begin{bmatrix} \mathbf{y} \\ -\mathbf{y} \\ \mathbf{b}_2 \\ -\mathbf{b}_1 \end{bmatrix}. \end{aligned}$$

After the solution $\mathbf{x}_{\ell_1}^*$ is found, the first $2K$ elements corresponding to \mathbf{x} are extracted and converted from real to complex to form the estimated data symbols.

¹Note that every Gram matrix is semidefinite positive [40, Theorem 7.2.10].

²The convexity of a function can be verified applying the second order conditions over the objective function; e.g., for problem (7), $\nabla^2 f(\mathbf{x}) = \mathbf{H}^T \mathbf{H} \succeq \mathbf{0}$.

2) LP WITH ℓ_∞ -NORM

Following a similar procedure, the LP detector based on ℓ_∞ norm is detailed. The cast to LP of the Chebyshev approximation [21] including the constellation symbol constraint becomes

$$\begin{aligned} & \underset{\mathbf{x}, t}{\text{minimize}} \quad t \\ & \text{s.t.} \quad -\mathbf{1}t \leq \mathbf{y} - \mathbf{H}\mathbf{x} \leq \mathbf{1}t \\ & \quad \mathbf{b}_1 \leq \mathbf{x} \leq \mathbf{b}_2. \end{aligned} \tag{11}$$

The problem (11) expressed in the *standard inequality form* is

$$\begin{aligned} & \underset{\mathbf{x}_{\ell_\infty}}{\text{minimize}} \quad \mathbf{c}_{\ell_\infty}^T \mathbf{x}_{\ell_\infty} \\ & \text{s.t.} \quad \mathbf{A}_{\ell_\infty} \mathbf{x}_{\ell_\infty} \leq \mathbf{b}, \end{aligned} \tag{12}$$

where:

$$\mathbf{c}_{\ell_\infty} = \begin{bmatrix} \mathbf{0} \\ \mathbf{1} \end{bmatrix}, \quad \mathbf{A}_{\ell_\infty} = \begin{bmatrix} \mathbf{H} & -\mathbf{1} \\ -\mathbf{H} & -\mathbf{1} \\ \mathbf{I} & \mathbf{0} \\ -\mathbf{I} & \mathbf{0} \end{bmatrix}, \quad \mathbf{x}_{\ell_\infty} = \begin{bmatrix} \mathbf{x} \\ t \end{bmatrix}.$$

After the solution $\mathbf{x}_{\ell_\infty}^*$ is found, the last element is discarded and the vector is converted from real to complex to form the estimated symbol obtained through the LP ℓ_∞ detector.

C. SEMIDEFINITE PROGRAMMING

The SDP is a powerful mathematical method [18] that has a competitive performance in MIMO detectors for high order modulations because of its polynomial worst-case complexity in contrast to ML that has an exponential complexity depending on the constellation size [17]. Here we consider [17] due to its simplicity and equivalence with other representations [20].

Considering the relaxation of the rank restriction in SDP formulation and the relaxation of the constellation symbols, it is possible to reformulate the detection problem for high-order modulation as the following SDP optimization problem [17]:

$$\begin{aligned} & \underset{\mathbf{X}}{\text{minimize}} \quad \text{trace}(\mathbf{L}\mathbf{X}) \\ & \text{s.t.} \quad \mathbf{X} \succeq \mathbf{0} \\ & \quad \mathbf{X}(N, N) = 1 \\ & \quad b_1^{\mathcal{B}^2} \leq \mathbf{X}(i, i) \leq b_2^{\mathcal{B}^2}, \end{aligned} \tag{13}$$

where \mathbf{X} is the $N \times N$ unknown variable, $N = 2K + 1$, the index $i = 1, \dots, N - 1$, scalars $b_1^{\mathcal{B}^2}$ and $b_2^{\mathcal{B}^2}$ represent the lower and upper limits of the set \mathcal{B}^2 (for example, 16-QAM has a set $\mathcal{B}^2 = \{1, 9\}$, so $b_1^{\mathcal{B}^2} = 1$ and $b_2^{\mathcal{B}^2} = 9$) and

$$\mathbf{L} = \begin{bmatrix} \mathbf{H}^T \mathbf{H} & -\mathbf{H}^T \mathbf{y} \\ -\mathbf{y}^T \mathbf{H} & 0 \end{bmatrix}. \tag{14}$$

The method considered here to extract the solution vector from \mathbf{X} is the rank-1 approximation [18],

$$\mathbf{x}_{\text{SDP}}^* = \mathbf{v}_1 \sqrt{\lambda_1}, \tag{15}$$

where λ_1 denotes the maximum eigenvalue and \mathbf{v}_1 is its associated eigenvector.

D. CLASSICAL LINEAR M-MIMO DETECTORS

For reference purpose, the classical linear detectors ZF and MMSE are considered and the estimated symbol is given in the form $\tilde{\mathbf{x}} = \mathbf{W}_{lin}\mathbf{y}$. The matrix \mathbf{W}_{lin} is expressed by:

$$\mathbf{W}_{lin} = \begin{cases} (\mathbf{H}^T \mathbf{H})^{-1} \mathbf{H}^T, & \text{ZF detector,} \\ \left(\mathbf{H}^T \mathbf{H} + \frac{\sigma_z^2}{E_s} \mathbf{I} \right)^{-1} \mathbf{H}^T, & \text{MMSE detector,} \end{cases} \quad (16)$$

with E_s denoting the symbol energy. The ZF M-MIMO detector is obtained performing the pseudoinverse of the channel matrix, while the MMSE M-MIMO detector requires the second order channel statistics.

IV. SOLVERS FOR CONVEX OPTIMIZATION

In this section, algorithms usually implemented in general purpose solvers for LP, QP and SDP formulations are discussed. Algorithms implemented more frequently in subsection IV-A and the TMP exploring the simple constraints is detailed in subsection IV-B.

A. INTERIOR-POINT METHODS

Interior point methods appeared as a polynomial complexity approach to solve LP problems with efficiency better than simplex [22]; those algorithms were extended and are also capable to solve QP problems [22]–[24] and also SDP problems [22].

Among different algorithms, for example, barrier method, primal-dual path following, and the affine scaling method, the MPC is one of the most efficient implementations [22], [23] in this category; in Matlab platform, it is implemented with commands *lsqlin* and *linprog* [28]–[30] to solve to solve QP and LP, respectively. For SDP, the CVX, a package for specifying and solving convex programs [42], [43], was considered in the numerical simulations configured to use the SDPT3 solver, which also employs an MPC implementation [31].

Interior point methods solve a linear system of equations at each iteration, and has similar computational complexity order compared with linear detectors [14], [44] and is more computationally intensive in the SDP case, where specialized interior-point algorithms for SDP may require $\mathcal{O}(K^{3.5})$ [18], [32].

Table 1 summarizes the number of unknowns, constraints and computational complexity order of each formulation. The SDP-based detector must find a matrix of unknowns, and is the most complex among the studied detectors. The number of unknowns in the LP ℓ_1 formulation depends on M , which is large in M-MIMO systems and this impacts on computational complexity. The number of unknowns is similar between QP and LP ℓ_∞ , however, as shown later in section V, the performance of QP is better than LP ℓ_∞ . The QP formulation presents the least number of unknowns and constraints and

TABLE 1. Problem size in terms of number of variables and constraints and the associated complexity for M-MIMO detectors.

| Detector | Variables | Constraints | Complexity |
|-----------------------|--------------|-------------|----------------------------------|
| QP (6) | $2K$ | $4K$ | $\mathcal{O}(N_{iter}K^3)$ |
| LP ℓ_1 (10) | $2K + 2M$ | $4M + 4K$ | $\mathcal{O}[N_{iter}(K + M)^3]$ |
| LP ℓ_∞ (12) | $2K + 1$ | $4M + 4K$ | $\mathcal{O}[N_{iter}(K + 1)^3]$ |
| SDP (13) | $(2K + 1)^2$ | $4K + 1$ | $\mathcal{O}(N_{iter}K^{3.5})$ |

is a good candidate to be an efficient detector with a good complexity-performance trade-off. In the next subsection, the application of TMP in the QP-based detector are detailed.

B. TWO-METRIC PROJECTION ALGORITHMS

The TMP method is of practical application when the projection on the feasible set can be carrier easily [33], such as the box constraints in the QP-based detector (6). We have considered an initial and feasible vector $\mathbf{x}_0 = \mathbf{0}$ in the middle of the feasible region (assuming a symmetric QAM constellation around zero, i.e. a 16-QAM with $\{\pm 1, \pm 3\}$).³ For different definitions of the direction matrix \mathbf{D} , we can obtain different algorithms, such as:

- 1) $\mathbf{D}_n = \mathbf{I}$, resulting in the PG method [26];
- 2) $\mathbf{D}_n = (\nabla^2 f(\mathbf{x}))^{-1} = (\mathbf{H}^T \mathbf{H})^{-1}$, the PN algorithm with complexity $2/3(2K)^3 + 2(2K)^2$ to perform LU factorization [21] for the matrix inverse calculation.
- 3) $\mathbf{D}_n = \frac{1}{\text{diag}(\nabla^2 f(\mathbf{x}))}$ scaling the gradient with the inverse of the diagonal, the Diagonally Scaled Projected Gradient (DSPG) method, which requires $2K$ flops after the precomputation of the Hessian;
- 4) Approximation of the inverse of the Hessian using Neumann series namely Projected Newton with Neuman Approximation (PNNA); under this approach it is affordable to consider 3 terms in the expansion resulting in cubic complexity [6] of $16K^3 + 12K^2 - 10$ flops.

Note that there are many possible variations, such as the approximation of Hessian (quasi-Newton method, e.g., BFGS [27]); approximations of the solution of the linear system of equations named truncated Newton; different line search algorithms can be employed beyond the Armijo-like rule, the utilization of an initial point (also called warm-start). Herein, we are not exhaustive, but trying promising combinations.

The steps of the TMP algorithm with the PN variation detailed in [25] are presented herein for completeness. When $\mathbf{D}_n = (\nabla^2 f(\mathbf{x}))^{-1}$ we have the PN; note the similarities when compared with the *unconstrained* counterpart NM: it is iterative, there is a search direction defined by matrix \mathbf{D}_n , a line search to find a step length α_n and an updating equation in a similar manner:

$$\mathbf{x}_{n+1}(\alpha_n) = [\mathbf{x}_n - \alpha_n \mathbf{D}_n \nabla f(\mathbf{x}_n)]^\#, \quad (17)$$

³Note that depending on the constraints, more sophisticated strategies may be required to choose a feasible initial point, for example, the solution of an LP [44].

with the operator $[.]^\#$

$$[a^i]^\# = \begin{cases} b_2^i & \text{if } b_2^i \leq a^i \\ a^i & \text{if } b_1^i < a^i < b_2^i \\ b_1^i & \text{if } a^i \leq b_1^i, \end{cases} \quad (18)$$

keeping the solution inside the feasible region (the box constraints). At the n th iteration, the matrix \mathbf{D}_n is diagonal with respect to subset of indexes $I_n^\#$ defined as

$$d^{ij} = 0, \quad \forall i \in I_n^\#, j \neq i, \quad (19)$$

and set of indexes are chosen such as

$$I_n^\# = \left\{ i \mid b_1^i \leq x_n^i \leq b_1^i + \varepsilon_n \text{ and } \frac{\partial f(\mathbf{x}_n)}{\partial x^i} > 0 \text{ or } \right. \\ \left. \times b_2^i - \varepsilon_n \leq x_n^i \leq b_2^i \text{ and } \frac{\partial f(\mathbf{x}_n)}{\partial x^i} < 0 \right\} \quad (20)$$

with tolerance

$$\varepsilon_n = \min\{\varepsilon, \|\mathbf{x}_n - \mathbf{M}_{\text{TM}} \nabla f(\mathbf{x}_n)\|_2\}, \quad (21)$$

where \mathbf{M}_{TM} is a definite positive diagonal matrix that can be fixed or vary at each iteration; herein, it was considered as \mathbf{I} as suggested in [25] for simplicity. The step length α_n is

$$\alpha_n = (\beta_{\text{TM}})^{m_n} \quad (22)$$

where m_n is the first m that attains the Armijo-like condition

$$f(\mathbf{x}_n) - f(\mathbf{x}(\beta_{\text{TM}}^m)) \geq \sigma_{\text{TM}} \left\{ \beta_{\text{TM}}^m \sum_{i \notin I_n^\#} \frac{\partial f(\mathbf{x}_n)}{\partial x^i} p_n^i \right. \\ \left. + \sum_{i \in I_n^\#} \frac{\partial f(\mathbf{x}_n)}{\partial x^i} [x_n^i - x_n^i(\beta_{\text{TM}}^m)] \right\} \quad (23)$$

and variables $\sigma_{\text{TM}} \in [0, 0.5]$, $\beta_{\text{TM}} \in [0, 1]$; m_n is nonnegative and

$$\mathbf{p}_n = \mathbf{D}_n \nabla f(\mathbf{x}_n). \quad (24)$$

The algorithm terminates when a critical point $\mathbf{x}_{n+1} = \mathbf{x}_n$ is found [25]. Numerically, here we consider that the algorithm terminates if the condition holds approximately in the form

$$\|\mathbf{x}_{n+1} - \mathbf{x}_n\|_2 \leq \varepsilon_n. \quad (25)$$

The mentioned steps are synthesized in Algorithm 1. After the stop criteria is attained, the solution vector \mathbf{x}_n is converted from real to complex form of the estimated data symbols. The computational complexity considered here is flops. Matrix and vector operations and some factorizations are found in [21, Appendix C]. Herein, the exponential operator $[.]^m$ and square root $\sqrt{[.]}$ (for calculation of ℓ_2 -norm) are counted as 8 flops; if conditions are ignored, for example in (18), since they are not mathematical operations such as sum, subtraction, division, multiplication in the definition of flop [45].

Similar terms in the objective function (7) and its gradient $\nabla f(\mathbf{x})$ can be precomputed and stored before entering Algorithm 1; a fixed computational cost in evaluating $\mathbf{H}^T \mathbf{H}$

Algorithm 1 Projected Newton Method for Problem (7)

- 1: Input parameters: $\sigma_{\text{pn}}, \beta_{\text{pn}}, \mathbf{D}_n, \mathbf{x}_0, \varepsilon, N_{\text{max}}, f(\mathbf{x}), \nabla f(\mathbf{x})$
- 2: Initialize $n = 0, \mathbf{x}_n = \mathbf{x}_0, \varepsilon_n$
- 3: **while** $n \leq N_{\text{max}}$ **do**
- 4: Evaluate and store $\nabla f(\mathbf{x}_n)$ $\triangleright 8K^2$
- 5: Evaluate tolerance (21) $\triangleright 20K$
- 6: Check indexes (20)
- 7: Zeroing some elements of \mathbf{D}_n eq.(19)
- 8: Evaluate (24) $\triangleright (4K^2 - 2K)$, or $2K$ if \mathbf{D}_n is diagonal
- 9: Line search (23) \triangleright
- $8K^2 + 6K - 2 + m_{\text{iter}}(8K^2 + 10K + 10)$
- 10: Next iteration point (17) $\triangleright 10K$
- 11: **if** condition (25) is attained **then**
- 12: Store n inside N_{iter}
- 13: **end if**
- 14: **end while**
- 15: Output: \mathbf{x}_n

results in $8K^2M - 4K$, the precomputation of $\mathbf{H}^T \mathbf{y}$ represents $8MK - 2K$ and the sum after the multiplication by \mathbf{x}_n spends $2K$ operations, resulting in a total of precomputation complexity of $\Upsilon_{\text{fixed}} = 8K^2M - 4K + 8MK$. The evaluation of the gradient $\nabla f(\mathbf{x}_n) = 2\mathbf{H}^T \mathbf{H} \mathbf{x}_n - 2\mathbf{H}^T \mathbf{y}$ requires only the evaluation of a matrix-vector multiplication of \mathbf{x}_n per iteration. Hence, the total computational complexity of each algorithm is composed by a fixed amount Υ_{fixed} plus the construction of \mathbf{D}_n and an iterative amount of operations described along Algorithm 1; the flops are summarized in Table 2, along with the flops count for linear detector MMSE, with N_{iter} representing the number of iterations till the condition (25) is attained and $m_{\text{iter}} = 1 + \bar{m}_n$, where \bar{m}_n is the mean number of m_n line search evaluations that attains the condition (23) plus one because $m = 0$ is the first evaluation.

Note that inside the projected algorithms only Υ_{fixed} depends on M ; equations inside Algorithm 1 involve the multiplication of matrices and vectors of size $2K$ and does not depend on M . The most costly part of the projected algorithms PN, PNNA, PG, DSPG applied to the M-MIMO detection is due to (23) calculation, which requires the evaluation of the objective function $N_{\text{iter}} m_{\text{iter}}$ times resulting in a complexity order of $\mathcal{O}(N_{\text{max}} m_n K^2)$.

The variable N_{iter} depends on the rate of convergence of each algorithm. PN is described as the fastest and PG the slowest among the studied projected algorithms; the rate of convergence of PG algorithm is given by [33]

$$\|\mathbf{x}_{n+1} - \mathbf{x}_{\text{QP}}^*\|_2 \leq \max\{\|1 - \alpha_n \lambda_{\text{min}}\|_1, \|1 - \alpha_n \lambda_{\text{max}}\|_1\} \|\mathbf{x}_n - \mathbf{x}_{\text{QP}}^*\|_2, \quad (26)$$

where λ_{min} and λ_{max} denote the minimum and maximum eigenvalues of the Hessian matrix and \mathbf{x}_{QP}^* is the optimal point for the QP formulation. Observing (26), the rate of convergence depends on the eigenvalues of the Hessian, which is the Gram matrix for QP, $\nabla^2 f(\mathbf{x}) = \mathbf{H}^T \mathbf{H}$. One can expect that changing the eigenvalues of the Hessian using different

TABLE 2. Number of flops for considered algorithms.

| M-MIMO Detector | Number of Operations |
|--|--|
| $\Upsilon_{\text{PN}}(K, M, N_{\text{iter}}, m_{\text{iter}})$ | $\Upsilon_{\text{fixed}} + \frac{16}{3}K^3 + 8K^2 + N_{\text{iter}}[20K^2 + 34K - 2 + m_{\text{iter}}(8K^2 + 10K + 10)]$ |
| $\Upsilon_{\text{PNNA}}(K, M, N_{\text{iter}}, m_{\text{iter}})$ | $\Upsilon_{\text{fixed}} + 16K^3 + 12K^2 - 10 + N_{\text{iter}}[20K^2 + 34K - 2 + m_{\text{iter}}(8K^2 + 10K + 10)]$ |
| $\Upsilon_{\text{PG}}(K, M, N_{\text{iter}}, m_{\text{iter}})$ | $\Upsilon_{\text{fixed}} + N_{\text{iter}}[16K^2 + 38K - 2 + m_{\text{iter}}(8K^2 + 10K + 10)]$ |
| $\Upsilon_{\text{DSPG}}(K, M, N_{\text{iter}}, m_{\text{iter}})$ | $\Upsilon_{\text{fixed}} + 2K + N_{\text{iter}}[16K^2 + 38K - 2 + m_{\text{iter}}(8K^2 + 10K + 10)]$ |
| $\Upsilon_{\text{MMSE}}(K, M)$ | $\Upsilon_{\text{fixed}} + \frac{16}{3}K^3 + 16K^2$ |

number of users $K \ll M$, the channel hardening effect occur changing the matrix condition number and influencing the rate of convergence of the projected algorithms. In that way, the number of iterations N_{iter} and evaluations m_{iter} are obtained numerically in order to characterize the full computational cost of the algorithm in section V.

Another detail to consider in the implementation is that the PN requires the Hessian to be definite positive and, in some scenarios, this condition may not be attained. So modifications in the Hessian matrix should be considered [22, Ch. 5], where the Hessian is replaced by

$$\widehat{\nabla^2 f(\mathbf{x})} = \frac{\nabla^2 f(\mathbf{x}) + \gamma \mathbf{I}}{1 + \gamma} \tag{27}$$

before the calculation of the inverse in the matrix \mathbf{D}_n for PN, where large values of the regularization factor γ approximates the NM to a Steepest Descent. The value of γ was determined through numerical simulations.

V. NUMERICAL RESULTS

Monte Carlo simulations (MCS) were carried out to demonstrate the effectiveness of the proposed detectors in terms of performance-complexity trade-off; all the MCS have been conducted under uncoded information scenarios. The reliability of the studied detectors are presented in subsection V-A, while the characterization and performance of the projected algorithms are presented in subsection V-B.

A. PERFORMANCE EVALUATION

The main M-MIMO system parameters considered are presented in Table 3. A default set of parameters appears on the top, and, for each scenario, one parameter is changed at time in order to observe its effect on the system performance. The optimization problems (6), (10), (12) were treated using Matlab optimization solvers, *lsqlin* and *linprog* commands for QP and LP, respectively. The problem (13) was solved using CVX, a package for specifying and solving convex programs [42], [43] configured to use the SDPT3 solver [31].

In Fig. 1, the BER performance for different values of signal-to-noise ratio (SNR) is presented for different detectors. Under uncorrelated scenarios and perfect CSI, the M-MIMO detectors with convex optimization formulation (LP, QP) presented better performance (lower BER) than linear detectors ZF and MMSE. Moreover, among the convex

TABLE 3. M-MIMO System and Channel MCS parameters.

| Parameter | Value |
|-------------------------------------|--|
| Number of BS antennas, M | 128 |
| Number of UE terminals, K | 128 |
| Modulation order | 16-QAM |
| Massive MIMO Detectors | Conventional: ZF, MMSE, LP ℓ_1 , LP ℓ_∞ , QP, SDP |
| LP, QP and SDP solver | <i>linprog</i> , <i>lsqlin</i> , CVX (SDPT3) |
| Channel condition ρ and τ | 0 |
| Scenarios | |
| Channel estimation quality, τ | [0; 0.05; 0.10] |
| Antenna correlation, ρ | [0; 0.5; 0.9] |
| Number of UE terminals, K | [128; 96; 64; 32] |
| Modulation order | [4; 16; 64] QAM |

detectors, QP provided the best performance, followed by LP ℓ_∞ and LP ℓ_1 formulations.

In Fig. 1a, considering errors in CSI around 5 and 10%, the BER performance was impaired for all detectors, while a similar behavior in performance compared to perfect CSI has been observed; SDP provides the best performance among analyzed detectors followed by QP, LP ℓ_1 , LP ℓ_∞ and linear detectors. Indeed, the linear detector ZF provides the poorest performance among the studied detectors; its performance is degraded even further with the increase of the τ parameter.

Fig. 1b exhibits the spatial antenna correlation impact on the BER performance; when $\rho = 0.5$, the overall performance is worsened; however, under extreme high correlated scenarios, i.e., $\rho = 0.9$, the performance of SDP, QP, LP ℓ_1 and LP ℓ_∞ is worse than MMSE, while the LP ℓ_1 detector exhibits similar performance compared to QP and SDP.

In Fig. 1c where the number of users are changed, the system loading $\frac{K}{M}$ is reduced progressively and the performance of linear detectors ZF and MMSE are significantly improved, surpassing LP ℓ_1 and LP ℓ_∞ detectors and providing performance similar to QP and SDP detectors; and a different behavior compared to previous scenarios (Figs. 1a and 1b) is observed among LP detectors: as the number of users is reduced, the performance of LP ℓ_1 surpasses LP ℓ_∞ .

In Fig. 1d, the modulation order was altered. In the low order modulation 4-QAM scenario, the improvement in performance of SDP compared with QP detector is more evident; performance of SDP and QP are better than linear detectors; moreover, the performance of LP ℓ_1 becomes very similar to LP ℓ_∞ , which is a different behavior compared with high

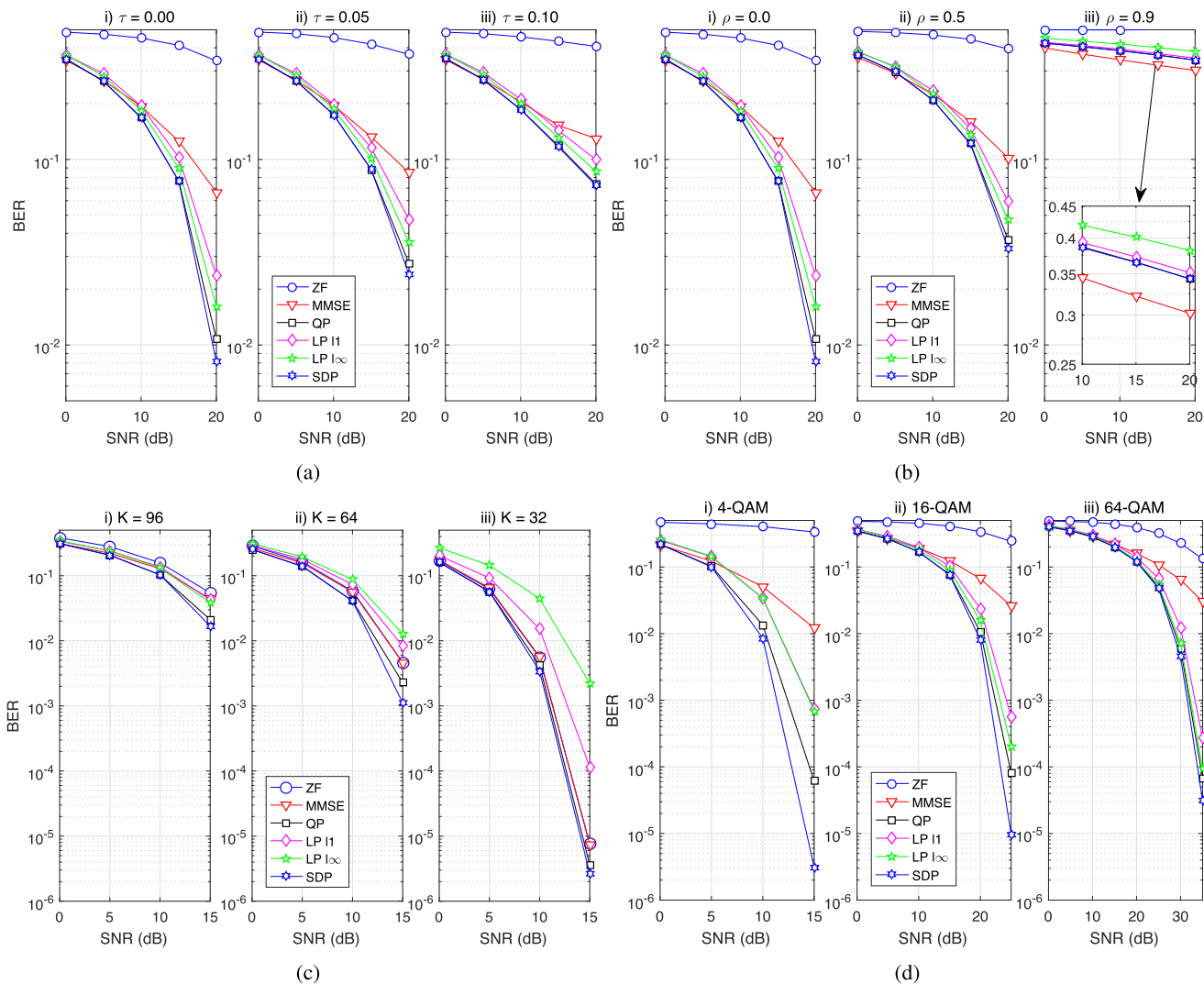


FIGURE 1. Performance of 128×128 M-MIMO detectors under realistic channel and intended system conditions: spatial correlation, error in the channel estimation and reduced number of users (system loading) and digital modulation order. (a) Performance with error in the channel estimation. (b) Performance with different correlation indexes. (c) Performance with different number of users. (d) Performance with different values of modulation order.

order modulations (16-QAM and 64-QAM), where $LP_{l\infty}$ provides superior performance compared with LP_{l1} .

In summary, although SDP provides the best performance, this advantage is not very distinguishable compared with QP performance with high order modulation, i.e., 16-QAM in Figs. 1a, 1b, and 1c; it is more prominent in 4-QAM presented in Fig. 1d. The QP detector provides suitable BER performance under scenarios with imperfect CSI, different system loading, at low or medium level of spatial correlation ($\rho \leq 0.5$) and only a slightly worse in performance than MMSE at the excessively correlated scenarios, i.e. $\rho = 0.9$. In the next subsection, projected algorithms are considered to solve the QP formulation in (7) focusing on the computational complexity while their solution quality and competitiveness are investigated and compared with the linear detector MMSE.

B. PROJECTED METHODS IN LS-MIMO DETECTION

In this subsection, MCS are performed focusing on computational complexity and characterization of parameters N_{iter} and m_{iter} in order to investigate the competitiveness of the projected algorithms applied to solve the QP formulation against linear detectors. The chosen scenarios are the ones that might interfere directly on the convergence properties as shown in (26): scenarios with different system loading $\frac{K}{M}$, including the intended use in LS-MIMO systems, where a large number of BS antennas serve a small number of users ($K \ll M$) and also when $K \approx M$ e.g., in crowded scenarios. First, numerical simulations were carried out in order to choose adequate input parameters for PG, DSPG, PNNA and PN algorithms. After that, the BER performance (deploying tuned parameters for a fair comparison) is computed and complexity compared in terms of flops. Finally, the performance

with different number of users but a constant system loading is performed, to further evidence that the number of iterations N_{iter} of projected algorithms depends mainly on the relation $\frac{K}{M}$ and the properties of the Hessian, but not so much on the dimensionality K of the QP problem.

1) DIFFERENT NUMBER OF USERS

Some algorithms are sensitive to the selection of input parameters, and an initial calibration may be required in order to improve the convergence speed. In [46], a methodology is proposed to tune the input parameters. Considering a certain interval for each parameter, one parameter is varied at time and the effect in performance is observed; the parameter that produces an adequate performance is chosen and the next input parameter is varied; two rounds of simulations are executed till the input parameters are chosen. Here, a similar procedure is deployed for $\gamma, \sigma_{TM}, \beta_{TM}, \varepsilon$ in order to characterize N_{iter} and m_{iter} for scenarios with different system loading. Considering an initial set of parameters depicted in Table 4, the procedure was executed first, for different system loading varying K , and after, for constant loading, changing both M and K .

TABLE 4. Scenario parameters for the calibration of input parameters for projected algorithms.

| Parameter | Value |
|--------------------------------------|---------------------|
| M | 128 |
| K | 128 |
| SNR | 15 dB |
| Detectors | QP, MMSE |
| Algorithms for QP | PN, PNNA, DSPG, PG |
| Initial Values | |
| ε | 10^{-2} |
| β_{TM}^{start} | 0.5 |
| σ_{TM}^{start} | 0.3 |
| N_{max}^{start} | 10 |
| γ^{start} | 0 |
| N_{max} | 5 |
| Intervals | |
| γ | $\in [0; 1.5]$ |
| β_{TM} | $\in [0.1; 0.9]$ |
| σ_{TM} | $\in [0.1; 0.4]$ |
| ε | $\in [0.5; 0.0001]$ |
| Scenarios | |
| Number of UE terminals, K | [128; 96; 64; 32] |
| Constant $\frac{K}{M} = \frac{1}{4}$ | $M = [128; 256]$ |

In Fig. 2, the influence of the regularization factor γ in (27) is observed, where the Hessian was substituted by $\nabla^2 f(\mathbf{x})$ before the computation of \mathbf{D}_n for PN and PNNA. The effect of γ is distinguishable in the scenario with $K = M$ for PN where the increase in γ results in better performance as shown in Fig. 2 i) and less line search evaluations depicted in Fig. 2 ii); after $\gamma = 1$ the improvements becomes smaller and so, $\gamma = 1$ is considered for PN in the $K = M$ scenario. Parameter γ does not seem to influence the performance for the other scenarios and other algorithms besides the PN, and also does not interfere in m_{iter} shown in 2 iii) for $K = 32$,

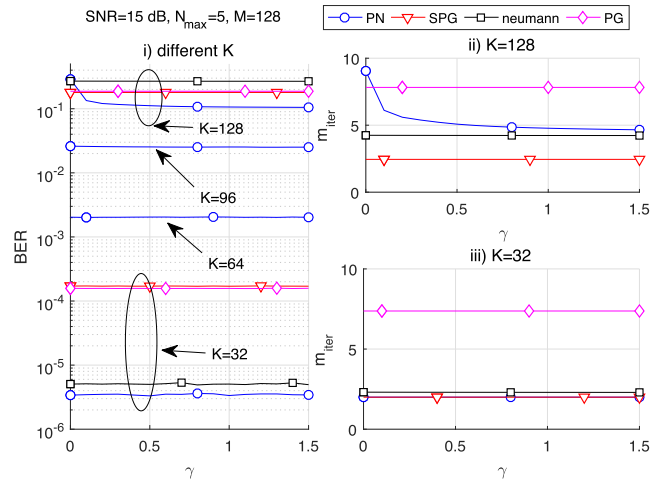


FIGURE 2. Influence of parameter γ for different simulation scenarios considered.

so the value $\gamma = 0$ is considered for other algorithms and other scenarios.

In Fig. 3, the calibration of parameters σ_{TM}, β_{TM} and ε are presented for $K = M$ and $K = \frac{M}{4}$; the procedure was also executed for $K = \frac{3M}{4}$ and $K = \frac{M}{2}$ but omitted herein for brevity. The left axis shows BER performance and the right axis the search evaluations m_{iter} , which impacts on the complexity. As β_{TM} increases, the evaluations of m_{iter} also increases, and more aggressively for PG. The parameter σ_{TM} is related to the step size in (22) and different values result in different performances for $K = 128$ and $K = 32$.

In the case of $\varepsilon, N_{max} = 5$ is not sufficient to achieve an MMSE performance for PG, DSPG and PNNA, and so, its effect is not clearly observed; the exception is the PN where the performance is slightly harmed when $\varepsilon = 0.5$. Therefore, the rate of convergence is characterized (parameters N_{iter} and m_{iter}), and a second round of simulations are executed with smaller values of ε . The information collected from the simulations illustrated in Fig. 3 and the two rounds for parameter ε shown in 4 is presented in Table 5.

Convergence for the M-MIMO detectors algorithms are presented in Fig. 4, where the BER performance is depicted as function of the number of iterations n . Adopted parameters are presented in Table 5. The number of iterations N_{iter} were stored in line 12 inside Algorithm 1 throughout the MCS and rounded; m_{iter} represents the line search evaluations, which is an internal step required to solve the optimization problem with projected methods and causes a direct impact on the number of flops in the final complexity are also presented. Observe that N_{iter} presented in the Table is also depicted inside Fig. 4. In Fig. 4a, the first round of ε is presented for the scenario with different number of users; details about the MMSE performance for each scenario are also presented. For DSPG, PNNA and PG, the performance is similar to MMSE, however, the value $\varepsilon = 0.5$ causes a premature termination of the algorithm since their performance could be improved with more iterations.

TABLE 5. Tuned parameters for the simulations with different number of users. The order is [PN; DSPG; PNNA; PG].

| Parameter | K=128 | K=96 | K=64 | K=32 |
|-------------------------|---------------------------|--------------------------|--------------------------|--------------------------|
| γ | [1; 0; 0; 0] | [0; 0; 0; 0] | [0; 0; 0; 0] | [0; 0; 0; 0] |
| β_{TM} | [0.5; 0.2; 0.4; 0.6] | [0.5; 0.4; 0.2; 0.2] | [0.5; 0.6; 0.3; 0.4] | [0.5; 0.3; 0.6; 0.3] |
| σ_{TM} | [0.3; 0.1; 0.1; 0.3] | [0.3; 0.4; 0.2; 0.1] | [0.3; 0.3; 0.1; 0.2] | [0.4; 0.2; 0.3; 0.1] |
| ε , round 1 | [0.5; 0.5; 0.5; 0.5] | [0.5; 0.5; 0.5; 0.5] | [0.5; 0.5; 0.5; 0.5] | [0.5; 0.5; 0.5; 0.5] |
| ε , round 2 | [0.5; 0.1; 0.1; 0.1] | [0.5; 0.1; 0.1; 0.1] | [0.1; 0.1; 0.1; 0.1] | [0.1; 0.1; 0.1; 0.1] |
| N_{iter} | [15; 29; 51; 37] | [6; 20; 23; 19] | [5; 15; 13; 12] | [3; 7; 6; 8] |
| m_{iter} | [6.49; 1.72; 4.01; 12.67] | [4.09; 2.11; 2.51; 4.63] | [2.89; 2.82; 2.40; 7.23] | [2.61; 1.70; 2.94; 5.64] |

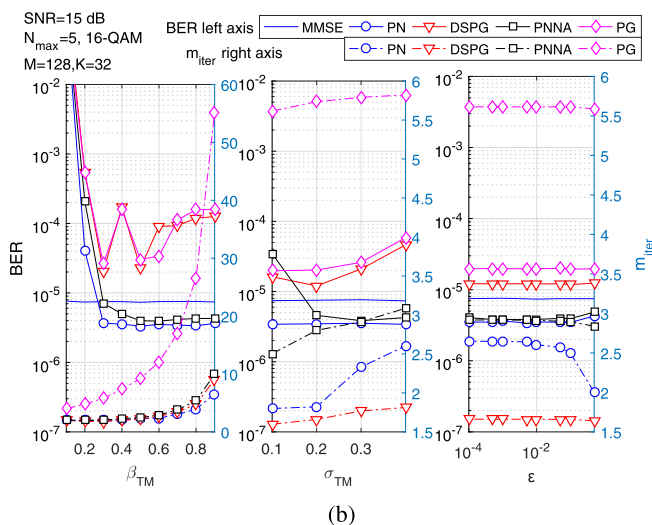
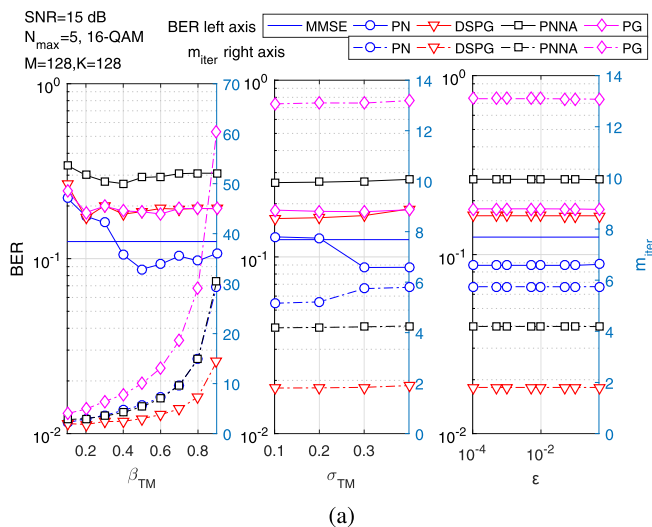


FIGURE 3. Performance varying the number of users in order to choose σ_{TM} , β_{TM} and ε parameters. (a) Calibration with users $K = M = 128$. (b) Calibration with users $K = \frac{1}{4}M = 32$.

In Fig. 4b, the convergence of the algorithms are compared. Two extreme situations are analyzed; the other scenarios $K = \frac{3}{4}M$ and $K = \frac{M}{2}$ are interpolations between them. A deeper analysis of the computational complexity in terms of flops is presented in section VI, where the complexity is compared with MMSE.

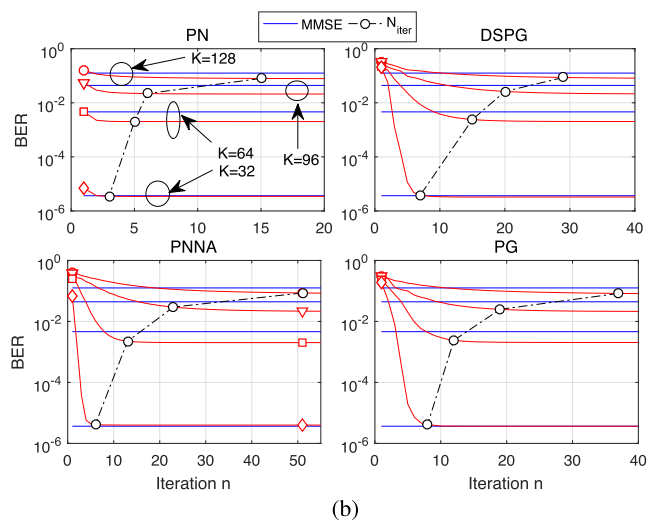
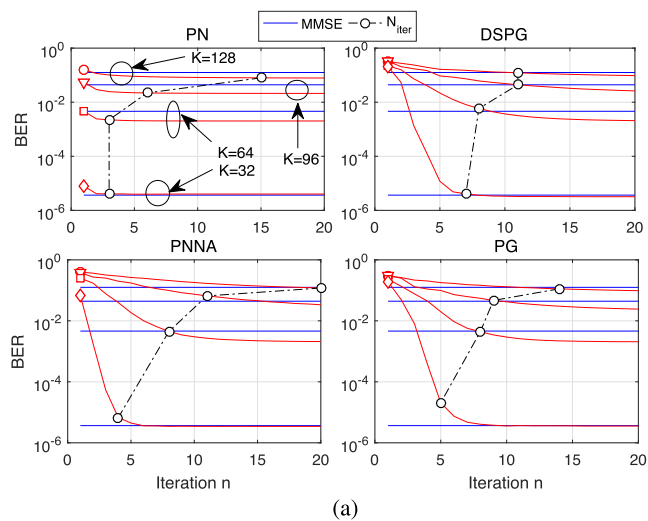


FIGURE 4. Rate of convergence of projected algorithms applied to QP formulation with different number of users. (a) Convergence considering values of ε for round 1. (b) Convergence considering values of ε for round 2.

- For $K = M = 128$, PN algorithm with ≈ 15 iterations can provide a better performance than MMSE with similar computational complexity order simply because it requires the calculation of the inverse of the Hessian. Neumann approximation for the inverse when $K \approx M$ is poor [6], and BER improvement of PNNA is slower than PG and DSPG. The PG and DSPG require a simpler D_n

TABLE 6. Tuned parameters for the simulations with constant system loading. The order is [PN; DSPG; PNNA; PG].

| Parameter | $M = 256, K = 64$ |
|---------------|---------------------------|
| γ | [0; 0; 0; 0] |
| β_{TM} | [0,5; 0,5; 0,5; 0,5] |
| σ_{TM} | [0,3; 0,2; 0,2; 0,2] |
| ε | [0,1; 0,1; 0,1; 0,1] |
| N_{iter} | [4; 8; 6; 8] |
| m_{iter} | [2,29; 2,11; 2,50; 10,11] |

matrix (PG an identity, DSPG a diagonal matrix) and after around 30 iterations, they achieve a performance similar to PN.

- For $K = 32 = \frac{M}{4}$, the performance of QP-based detectors is almost the same achieved by the MMSE, as shown previously in Fig.1c; the number of iterations to achieve MMSE performance is reduced for all algorithms. For PN, around 4 iterations are required. Neumann approximation becomes more accurate with the reduction of $\frac{K}{M}$ [6]; in such low system loading scenario, the convergence of PNNA is substantially improved in comparison with $K = 128$, and less than 10 iterations are enough to provide MMSE-like BER; for PG and DSPG, less than 10 iterations are sufficient to achieve MMSE-like performance.

2) CONSTANT SYSTEM LOADING

Here, simulations considering a constant system loading are presented in order to observe the behavior of the projected algorithms when the dimensionality of the problem increases (more users, more unknown variables in the QP problem), while keeping a constant (and low) system loading of $\frac{K}{M} = \frac{1}{4}$ aiming to maintain the characteristic of the channel hardening, i.e., a well-conditioned Hessian $\mathbf{H}^T \mathbf{H}$.

The convergence considering a constant system loading $\frac{K}{M} = \frac{1}{4}$ is presented in Fig. 5. The procedure considered in the previous simulations are also deployed here. The input parameters σ_{TM} , β_{TM} and ε are determined through numerical simulations as shown in Fig. 5a and condensed in Table 6, and the number of iterations N_{iter} and line search evaluations m_{iter} are obtained numerically; the N_{iter} is shown in Fig. 5b. A similar behavior is observed in the scenario 128×32 (from previous subsection) and 256×64 ; a reduced number of iterations (less than 10) are required for the projected algorithms and is an indicative that the method works in larger systems without great impacts on the number of iterations and, consequently, in complexity.

Considering the values of N_{iter} and m_{iter} obtained, the computational complexity is further characterized in the next section.

VI. COMPUTATIONAL COMPLEXITY

The computational complexity is analyzed in two parts. In the first, SDP, QP, LP ℓ 1 and LP ℓ ∞ are compared in terms of complexity order; in the second part, the projected algorithms

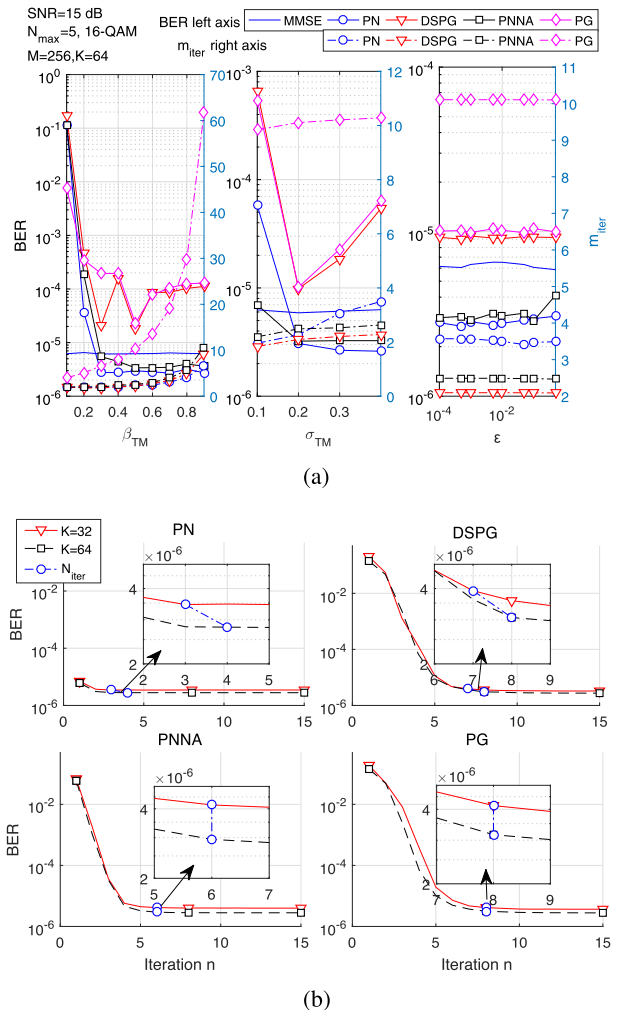


FIGURE 5. Convergence and line search evaluations considering different number of BS and UE antennas, keeping the system loading $\frac{K}{M}$ constant. (a) Calibration of input parameters for constant system loading. (b) Convergence for a constant system loading $\frac{1}{4}$, $M = 128$ and $M = 256$ with SNR = 15dB.

are evaluated in terms of flops and compared with the linear detector MMSE.

Initially, a complexity comparison considering SDP, QP, LP ℓ 1, LP ℓ ∞ and linear detectors presented in subsection V-A is considered using complexity metric given in terms of \mathcal{O} (big-O) notation, as shown in Table 1. The complexity per iteration of SDP is the biggest, followed by LP ℓ 1; LP ℓ ∞ and QP. The number of iterations for each detector evaluated numerically is presented in Table 7. Combining the information presented in those two tables, the SDP-based detector provides a good performance with a high complexity cost: each iteration costs more and N_{iter} is also greater than other detectors. LP ℓ 1 presents a cost per iteration higher, however costs ≈ 3 iterations less than LP ℓ ∞ . Regard QP, its complexity per iteration is lower and requires fewer N_{iter} than other detectors providing suitable trade-off among the performance of the studied M-MIMO detectors.

TABLE 7. Number of iterations for different detectors under the condition SNR = 15 dB.

| Detectors | 4-QAM | 16-QAM | 64-QAM |
|-----------|-------|--------|--------|
| LPℓ1 | 15.35 | 14.11 | 13.25 |
| LPℓ∞ | 17.24 | 16.49 | 16.04 |
| QP | 7.88 | 9.55 | 9.02 |
| SDP | 16.72 | 21.74 | 23.62 |

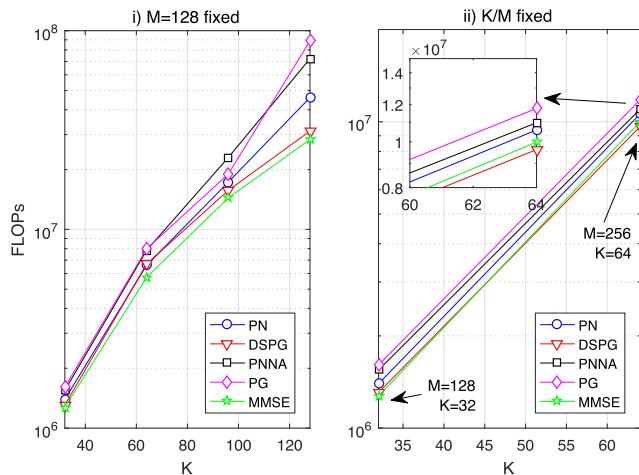


FIGURE 6. Number of flops for the LS-MIMO detectors considering different system loading varying K users, and with a constant K/M , increasing both UE and BS antennas.

Regard the impact of the modulation order, for SDP, N_{iter} increased for higher orders, however this behavior was not observed for other detectors; only small fluctuations were observed. For QP, N_{iter} was around 8 to 9 iterations; for LPℓ∞ around 16 and 17 and for LPℓ1, N_{iter} presented a small reduction around 2 iterations (from 15 to 13) as the modulation order increased.

In the second part, a more in-depth computational complexity analysis for the projected algorithms described in section V-B is developed considering the number of flops. Using expressions from Table 2 and substituting the respective number of iterations N_{iter} and line search evaluations m_{iter} obtained in subsection V-B, the plots presented in Fig. 6 are obtained.

From Fig. 6 i) with $K = 32$, MMSE provides the lowest number of flops. Although PG and DSPG have a diagonal \mathbf{D}_n matrix and similar N_{iter} , the DSPG requires a lower m_{iter} than PG, hence, a lower number of flops. PN presented a low N_{iter} however it also requires a matrix inverse computation resulting in more complexity compared with MMSE. Finally, Neumann approximation is poor for large K and PNNA presented a slow convergence (high N_{iter}) resulting in higher complexity compared with PN approach.

In Fig. 6 ii), the number of flops considering a constant system loading is presented. Observing the flop-complexity

expressions, the matrix-vector operations required for MMSE (Υ_{fixed}) are also required for the other algorithms, and the projected algorithms evaluates K^2 operations $N_{iter}m_{iter}$ times. So, the complexity order of MMSE and projected algorithms, now considering the \mathcal{O} notation, is $\mathcal{O}(K^3)$ and $\mathcal{O}(N_{iter}m_{iter}K^2)$, respectively. Keeping the proportion $\frac{K}{M} = \frac{1}{4}$, the computational complexity order of DSPG would be lower than MMSE when $N_{iter}m_{iter} < K$. Indeed, we see that the number of iterations does not affect too much $N_{iter}m_{iter}$; hence, as K increases, the computational complexity approaches the MMSE complexity. Evaluating in terms of flops, the computational complexity for DSPG was lower than MMSE for $M = 256$ and $K = 64$; in other words, DSPG provides good BER performance with low computational complexity in terms of flops.

VII. CONCLUSIONS AND REMARKS

In the first part of this work, M-MIMO detectors using four promising optimization formulations, namely LPℓ1, LPℓ∞, QP and SDP are analyzed considering high-order modulation in realistic scenarios including spatial correlation, error in CSI, different system loading and modulation order. The SDP detector provided the best performance among the studied detectors in a variety of scenarios; the exception was the excessively high correlated scenario, $\rho = 0.9$, where the performance of all detectors were severely degraded, and MMSE provided a slightly better performance. The LPℓ∞ provided lower computational complexity per iteration compared with LPℓ1 and a better performance under imperfect CSI and medium correlation $\rho = 0.5$; however, a worse performance for different system loading ($K = 64$ and $K = 32$), and similar performance for the low-order modulation 4-QAM. The QP detector showed the lowest complexity order per iteration and also better performance compared with both LPℓ1 and LPℓ∞.

In the second part, projected algorithms, which explore simple constraints of the formulated problem, were applied to find the transmitted symbols of a M-MIMO detector written as a QP problem. A methodology to determine the line search parameters was applied and, through numerical simulations, the improvements in the rate of convergence of the algorithms (reduction of N_{iter}) due to the well-conditioned Gram matrix (channel hardening) were evidenced; the convergence is slower for $K \approx M$ than for $K \ll M$. The computational complexity order of MMSE and projected algorithms are $\mathcal{O}(K^3)$ and $\mathcal{O}(N_{iter}m_{iter}K^2)$, respectively. The use of projected algorithms is suggested in scenarios where $N_{iter}m_{iter} < K$, noting that N_{iter} increases slowly as K increases while $\frac{K}{M} = \frac{1}{4}$, as observed during numerical simulations with $K = 32, M = 128$ and $K = 64, M = 256$. Hence, QP solved with DSPG provided better performance than MMSE in scenarios with $K \approx M$ and showed promising computational complexity for scenarios with increasing K and low system loading.

REFERENCES

- [1] T. L. Marzetta, "Noncooperative cellular wireless with unlimited numbers of base station antennas," *IEEE Trans. Wireless Commun.*, vol. 9, no. 11, pp. 3590–3600, Nov. 2010.
- [2] E. G. Larsson, O. Edfors, F. Tufvesson, and T. L. Marzetta, "Massive MIMO for next generation wireless systems," *IEEE Commun. Mag.*, vol. 52, no. 2, pp. 186–195, Feb. 2014.
- [3] S. Yang and L. Hanzo, "Fifty years of MIMO detection: The road to large-scale MIMOs," *IEEE Commun. Surveys Tuts.*, vol. 17, no. 4, pp. 1941–1988, 4th Quart., 2015.
- [4] F. Rusek *et al.*, "Scaling up MIMO: Opportunities and challenges with very large arrays," *IEEE Signal Process. Mag.*, vol. 30, no. 1, pp. 40–60, Jan. 2013.
- [5] A. Chockalingam and B. S. Rajan, *Large MIMO Systems*. New York, NY, USA: Cambridge Univ. Press, 2014.
- [6] M. Wu, B. Yin, G. Wang, C. Dick, J. R. Cavallaro, and C. Studer, "Large-scale MIMO detection for 3GPP LTE: Algorithms and FPGA implementations," *IEEE J. Sel. Topics Signal Process.*, vol. 8, no. 5, pp. 916–929, Oct. 2014.
- [7] L. Dai, X. Gao, X. Su, S. Han, C.-L. I, and Z. Wang, "Low-complexity soft-output signal detection based on Gauss-Seidel method for uplink multiuser large-scale MIMO systems," *IEEE Trans. Veh. Tech.*, vol. 64, no. 10, pp. 4839–4845, Oct. 2015.
- [8] V. Gupta, A. K. Sah, and A. K. Chaturvedi, "High precision low complexity matrix inversion based on Newton iteration for data detection in the massive MIMO," *IEEE Commun. Lett.*, vol. 20, no. 3, pp. 490–493, Mar. 2016.
- [9] Y. Wang and H. Leib, "Sphere decoding for MIMO systems with Newton iterative matrix inversion," *IEEE Commun. Lett.*, vol. 17, no. 2, pp. 389–392, Feb. 2013.
- [10] J. Minango and C. de Almeida, "Low complexity zero forcing detector based on Newton-schultz iterative algorithm for massive MIMO systems," *IEEE Trans. Veh. Technol.*, vol. 67, no. 12, pp. 11759–11766, Dec. 2018.
- [11] M. Mandloi and V. Bhatia, "Low-complexity near-optimal iterative sequential detection for uplink massive MIMO systems," *IEEE Commun. Lett.*, vol. 21, no. 3, pp. 568–571, Mar. 2017.
- [12] T. Cui, T. Ho, and C. Tellambura, "Linear programming detection and decoding for MIMO systems," in *Proc. IEEE Int. Symp. Inf. Theory*, Jul. 2006, pp. 1783–1787.
- [13] Y. Hashimoto, K. Konishi, T. Takahashi, K. Uruma, and T. Furukawa, "L1 norm minimization approach to MIMO detector," in *Proc. 8th Int. Conf. Signal Process. Commun. Syst. (ICSPCS)*, Dec. 2014, pp. 1–4.
- [14] A. Elghariani and M. Zoltowski, "Low complexity detection algorithms in large-scale MIMO systems," *IEEE Trans. Wireless Commun.*, vol. 15, no. 3, pp. 1689–1702, Mar. 2016.
- [15] Y. H. Zhang, W.-S. Lu, and T. A. Gulliver, "Integer QP relaxation-based algorithms for intercarrier-interference reduction in OFDM systems," *Can. J. Elect. Comput. Eng.*, vol. 32, no. 4, pp. 199–205, 2007.
- [16] F. A. Bhatti, S. A. Khan, S. U. Rehman, and F. Rasool, "MIMO OFDM signal detection using quadratic programming," in *Proc. IEEE 14th Int. Multitopic Conf.*, Dec. 2011, pp. 323–328.
- [17] N. D. Sidiropoulos and Z.-Q. Luo, "A semidefinite relaxation approach to MIMO detection for high-order QAM constellations," *IEEE Signal Process. Lett.*, vol. 13, no. 9, pp. 525–528, Sep. 2006.
- [18] Z.-Q. Luo, W.-K. Ma, A. M.-C. So, Y. Ye, and S. Zhang, "Semidefinite relaxation of quadratic optimization problems," *IEEE Signal Process. Mag.*, vol. 27, no. 3, pp. 20–34, May 2010.
- [19] J. L. Negrão, A. M. Mussi, and T. Abrão, "Semidefinite relaxation for large scale MIMO detection," in *Proc. XXXIV Simp. Br. Telecom.-SBRT2016*, Sep. 2016, pp. 324–328.
- [20] W.-K. Ma, C.-C. Su, J. Jalden, T.-H. Chang, and C.-Y. Chi, "The equivalence of semidefinite relaxation MIMO detectors for higher-order QAM," *IEEE J. Sel. Topics Signal Process.*, vol. 3, no. 6, pp. 1038–1052, Dec. 2009.
- [21] S. Boyd and L. Vandenberghe, *Convex Optimization*. New York, NY, USA: Cambridge Univ. Press, 2004.
- [22] A. Antoniou and W.-S. Lu, *Practical Optimization: Algorithms and Engineering Applications*, 1st ed. New York, NY, USA: Springer, 2007.
- [23] J. Nocedal and S. Wright, *Numerical Optimization* (Springer Series in Operations Research and Financial Engineering). New York, NY, USA: Springer-Verlag, 2006.
- [24] J. Gondzio, "Interior point methods 25 years later," *Eur. J. Oper. Res.*, vol. 218, no. 3, pp. 587–601, 2012.
- [25] D. P. Bertsekas, "Projected newton methods for optimization problems with simple constraints," in *Proc. 20th IEEE Conf. Decis. Control Including Symp. Adapt. Processes*, Dec. 1981, pp. 762–767.
- [26] M. Schmidt, D. Kim, and S. Sra, *Projected Newton-Type Methods in Machine Learning*. Cambridge, MA, USA: MIT Press, Dec. 2011, pp. 305–330.
- [27] D. Kim, S. Sra, and I. S. Dhillon, "Tackling box-constrained optimization via a new projected quasi-Newton approach," *SIAM J. Sci. Comput.*, vol. 32, no. 6, pp. 3548–3563, 2010.
- [28] Matlab. *Lsqlin: Solve Constrained Linear Least-Squares Problems*. Accessed: Nov. 18, 2018. [Online]. Available: <https://www.mathworks.com/help/optim/ug/lsqlin.html>
- [29] *Quadratic Programming Algorithms*. Accessed: Nov. 18, 2018. [Online]. Available: <https://www.mathworks.com/help/optim/ug/quadratic-programming-algorithms.html>
- [30] *Linprog: Solve Linear Programming Problems*. Accessed: Nov. 18, 2018. [Online]. Available: <https://www.mathworks.com/help/optim/ug/linprog.html>
- [31] R. H. Tütüncü, K. C. Toh, and M. J. Todd, "Solving semidefinite-quadratic-linear programs using SDPT₃," *Math. Program.*, vol. 95, no. 2, pp. 189–217, Feb. 2003.
- [32] W.-K. Ma, C.-C. Su, J. Jalden, and C.-Y. Chi, "Some results on 16-QAM MIMO detection using semidefinite relaxation," in *Proc. IEEE Int. Conf. Acoust., Speech Signal Process.*, Mar./Apr. 2008, pp. 2673–2676.
- [33] D. P. Bertsekas, *Nonlinear Programming*, 2nd ed. Belmont, MA, USA: Athena Scientific, 1999.
- [34] J.-C. Chen, "Gradient projection-based alternating minimization algorithm for designing hybrid beamforming in millimeter-wave MIMO systems," *IEEE Commun. Lett.*, vol. 23, no. 1, pp. 112–115, Jan. 2019.
- [35] J. Chen, Z. Zhang, H. Lu, J. Hu, and G. E. Sobelman, "An intra-iterative interference cancellation detector for large-scale MIMO communications based on convex optimization," *IEEE Trans. Circuits Syst. I, Reg. Papers*, vol. 63, no. 11, pp. 2062–2072, Nov. 2016.
- [36] J. R. Hampton, *Introduction to MIMO Communications*. New York, NY, USA: Cambridge Univ. Press, 2014.
- [37] V. Zelst and J. Hammerschmidt, "A single coefficient spatial correlation model for multiple-input multiple-output (MIMO) radio channels," in *Proc. 27th Gen. Assem. Int. Union Radio Sci. (URSI)*, no. 1, 2002, pp. 2–5.
- [38] R. Couillet and M. Debbah, *Random Matrix Methods for Wireless Communications*. Cambridge, U.K.: Cambridge Univ. Press, 2011.
- [39] P. L. De Angelis, P. M. Pardalos, and G. Toraldo, *Quadratic Programming with Box Constraints*. Boston, MA, USA: Springer, 1997, pp. 73–93.
- [40] R. A. Horn and C. R. Johnson, *Matrix Analysis*, 2nd ed. New York, NY, USA: Cambridge Univ. Press, 2012.
- [41] P. M. Pardalos and S. A. Vavasis, "Quadratic programming with one negative eigenvalue is NP-hard," *J. Global Optim.*, vol. 1, no. 1, pp. 15–22, Mar. 1991.
- [42] M. Grant and S. Boyd. (Mar. 2014). *CVX: MATLAB Software for Disciplined Convex Programming, Version 2.1*. [Online]. Available: <http://cvxr.com/cvx>
- [43] M. C. Grant and Stephen P. Boyd, "Graph implementations for non-smooth convex programs," in *Recent Advances in Learning and Control* (Lecture Notes in Control and Information Sciences), V. Blondel, S. P. Boyd, and H. Kimura, Eds. Berlin, Germany: Springer-Verlag, 2008, pp. 95–110.
- [44] M. S. K. Lau, S. P. Yue, K. V. Ling, and J. M. Maciejowski, "A comparison of interior point and active set methods for FPGA implementation of model predictive control," in *Proc. Eur. Control Conf. (ECC)*, Aug. 2009, pp. 156–161.
- [45] G. H. Golub and C. F. Van Loan, *Matrix Computations*, 4th ed. Baltimore, MD, USA: Johns Hopkins Univ. Press, 2013.
- [46] J. C. M. Filho, R. N. de Souza, and T. Abrão, "Ant colony input parameters optimization for multiuser detection in DS/CDMA systems," *Expert Syst. Appl.*, vol. 39, no. 17, pp. 12876–12884, 2012.



RAFAEL MASASHI FUKUDA received the B.S. degree in electrical engineering from the State University of Londrina, Brazil, in 2017, where he is currently pursuing the M.Sc. degree in electrical engineering. His research interests include OFDM and MIMO systems, 4G and 5G wireless systems, signal processing, and heuristics and convex optimization techniques for wireless communication systems.



TAUFIK ABRÃO (M'01–SM'12) received the B.S., M.Sc., and Ph.D. degrees in electrical engineering from the Polytechnic School of the University of São Paulo, Brazil, in 1992, 1996, and 2001, respectively. Since 1997, he has been with the Communications Group, Department of Electrical Engineering, State University of Londrina, Brazil, where he is currently an Associate Professor in telecommunications and the Head of the Telecommunications and Signal Processing Laboratory.

From 2007 to 2008, he was a Postdoctoral Researcher with the Department of Signal Theory and Communications, Polytechnic University of Catalonia, Spain. In 2012, he was an Academic Visitor with the Southampton Wireless Research Group, University of Southampton, U.K. He has participated in several projects funded by government agencies and industrial companies. He has supervised 24 M.Sc. and four Ph.D. students and two Postdocs and has co-authored nine book chapters on mobile radio communications and over 180 research papers published in specialized/international journals and conferences. His current research interests include communications and signal processing, especially multiuser detection and estimation, MC-CDMA and MIMO systems, cooperative communication and relaying, resource allocation, and the heuristic and convex optimization aspects of 3G and 4G wireless systems. He is a member of SBrT. He is involved in the Editorial Board activities of six journals in telecommunications area and has served as a TPC Member of several symposiums and conferences. He has been serving as an Editor for the IEEE COMMUNICATIONS SURVEYS AND TUTORIALS, since 2013, the IEEE ACCESS, since 2016, the *IET Journal of Engineering*, since 2014, and ETT-Wiley, since 2016.

• • •